ARTHROPOD SYSTEMATICS & PHYLOGENY

76 (2): 295–302
18.7.2018

SENCKENBERG

Cenozoic out-of-Africa dispersal shaped diversification of the whirligig beetle genus *Aulonogyrus* (Coleoptera: Gyrinidae: Gyrinini)

Grey T. Gustafson

Department of Ecology and Evolutionary Biology, and Division of Entomology, Biodiversity Institute, University of Kansas, Lawrence, KS 66045, USA [gtgustafson@gmail.com]

Accepted 28.iii.2018.
Published online at www.senckenberg.de/arthropod-systematics on 29.vi.2018.
Editors in charge: Christiane Weirauch & Klaus-Dieter Klass

Abstract. The whirligig beetle genus *Aulonogyrus* Motschulsky, 1853 comprises more than fifty species divided among five subgenera. The genus has high endemicity in southern Africa, with additional endemic species found on Madagascar, Australia, and New Caledonia. This distribution has been proposed to be of Gondwanan origin. In Africa and Madagascar, species of *Aulonogyrus* are relatively common freshwater macroinvertebrates inhabiting a variety of lotic and lentic habitats. The phylogenetic relationships and historical biogeography of the genus have never been examined, and it has been suggested that subgenera of *Aulonogyrus* are not natural groups. Here both Bayesian and maximum likelihood phylogenetic inference are conducted on the genus using data from six gene fragments to reconstruct the evolutionary history of the group. Ancestral range reconstructions are performed to infer the historical biogeography of the genus. Strong support for the monophyly of the genus *Aulonogyrus* and the subgenera *Aulonogyrus* s.str. and *Afrogyrus* Brinck, 1955 was recovered. The three Malagasy subgenera are synonymized with the primarily African subgenus *Afrogyrus*: *Pterygyrus* Brinck, 1955 **n.syn.**, *Lophogyrus* Brinck, 1955 **n.syn.**, and *Paragyrus* Brinck, 1955 **n.syn.** The ancestral range reconstruction supports an African origin for the genus with several independent Cenozoic out-of-Africa dispersal events to Madagascar, and the Palearctic and Oceania regions resulting in its current distribution.

Key words. Phylogeny, classification, biogeography, aquatic beetles.

1. Introduction

The whirligig beetle genus *Aulonogyrus* Motschulsky, 1853 comprises 54 species of medium-sized (4–10.5 mm) aquatic beetles, found primarily within the Ethiopian region (Brinck 1955a). Notably, the genus has high endemic diversity in southern Africa, as well as four endemic species occurring on Madagascar (Legros 1951; Brinck 1955a), a single widespread Australian species (Watts & Hamon 2010), and another one found on New Caledonia (Mazzoldi 2010). In Africa and Madagascar, members of *Aulonogyrus* are relatively common, being found on a variety of freshwater bodies from temporary pools and streams in coastal and arid regions, to permanent, large, tropical rivers, and even high-elevation mountain streams (Brinck 1955b). The distribution of *Aulonogyrus* has been interpreted by some workers as being Gondwanan, with speculation that the genus (Hatch 1926) and its Australasian species originated prior to the southern supercontinent's breakup (Ochs 1949). However, in a recent study on the diversification of the Gyrinidae, Gustafson et al. (2017) found that the crown Gyrinini originated in the Late Cretaceous, rendering a Gondwanan vicariance scenario highly unlikely. Other researchers have instead favored dispersal as best explaining this distribution (Brinck 1955b), with the Australasian species representing a relatively young lineage (Brinck 1955a). All previous researchers agreed the origin of the group likely lay within the Ethiopian region (Hatch 1926; Ochs 1949; Brinck 1955a,b).

Within *Aulonogyrus* two distinct groups of species are apparent: those with the lateral margins of the elytra

and pronotum darkly colored (similar to the pronotal and elytral discs) and are found in lentic habitats; and species with lightly-colored, yellow lateral margins which are largely found in lotic habitats (RÉGIMBART 1883; BRINCK 1955b). A few species of *Aulonogyrus* can be found in both habitats (e.g. *A. algoensis* Régimbart, 1883) (BRINCK 1955b). It has been proposed that the dark-margined, lentic species represent the earliest diverging lineage within the genus (HATCH 1926; OCHS 1949). BRINCK (1955a,b), while agreeing with this view, thought the dark-margined species did not form a monophyletic group, instead he suggested yellow-margins evolved multiple times within different lineages of *Aulonogyrus* and that inhabiting the lotic environments of southern Africa represented a derived condition. BRINCK (1955a), who most recently revised the genus, formally divided it into five subgenera, separating the four Malagasy species into three subgenera, grouping the African species along with the single Indian / Sri Lankan species into the subgenus *Afrogyrus* Brinck, 1955a, and placing the species from the Palearctic and Oceania regions into the *Aulonogyrus* s.str. subgenus. The genus *Aulonogyrus* has never been the specific subject of phylogenetic analysis and the monophyly of the proposed subgenera have never been tested.

The goal of this study is to conduct the first phylogenetic analyses on the genus in order to (1) assess the monophyly of the subgenera and revise the classification if necessary; (2) construct a time calibrated phylogeny to reconstruct the evolutionary history of the genus and provide timing for its diversification; (3) reconstruct ancestral ranges occupied by the genus to elucidate its historical biogeography.

2. Material and methods

2.1. Data

Taxon sampling. The dataset for this study included 36 species of Gyrinidae (Table S1). Outgroup sampling comprised three members of the Dineutini, two Orectochilini, six *Gyrinus* Geoffroy, 1762 species, and one species of *Metagyrinus* Brinck, 1955a. For ingroup taxa a total of 24 species of *Aulonogyrus* were sampled from all five of the currently recognized subgenera. Subgeneric sampling consisted of three of the four known species of *Aulonogyrus* s.str.; 16 of the 45 species of *Afrogyrus*; both species of *Lophogyrus* Brinck, 1955a; and the two monotypic subgenera *Paragyrus* Brinck, 1955a and *Pterygyrus* Brinck, 1955a.

Molecular data. Thoracic muscle tissue was removed from specimens preserved in 95% ethanol via a lateral incision using fine-tip forceps. When there was little thoracic muscle tissue to extract (i.e. teneral individuals or smaller species), one of the fore- or middle legs was also removed. DNA was extracted using a QIAGEN DNEasy kit (Valencia, CA, USA) and the protocol for animal tissue.

Polymerase chain reaction protocols from WILD & MADDISON (2008) and MILLER & BERGSTEN (2012) were followed to amplify and then sequence the following gene fragments: *cytochrome oxidase subunit I* (COI, 1281 bp aligned), *cytochrome oxidase subunit II* (COII, 684 bp aligned), *12S rRNA* (12S, 359 bp aligned), *28S rDNA* (28S, 1266 bp aligned), *histone III* (H3, 330 bp aligned), and *arginine kinase* (AK, 723 bp aligned). Primers used for amplification and sequencing are included along with their sources in Table S2. Gene fragment coverage for each taxon in the analysis is provided in Table S1. Sequences were edited using GENEIOUS R10.2.2 (Biomatters, https://www.geneious.com) and aligned using MUSCLE (EDGAR 2004). Cleaning of sequences, frame checking, and concatenation was done in Mesquite 3.10 (MADDISON & MADDISON 2015).

Partitioning. To find the partitioning scheme of the molecular data for phylogenetic analysis, PartitionFinder 1.1.1 (LANFEAR et al. 2012) was run on the concatenated dataset under the 'greedy' search algorithm, with unlinked branch-lengths, and Akaike information criterion corrected (AICc) model selection.

2.2. Phylogenetic analyses

Bayesian inference. Bayesian analyses were implemented using the MPI version of MrBayes 3.2.6 (RONQUIST et al. 2012b; ZHANG et al. 2016). No substitution model was selected *a priori*; instead, the reversible-jump Markov chain Monte Carlo (MCMC) method with gamma-distributed rate variation across sites was used to test the probability of different models *a posteriori* during analysis (HUELSENBECK et al. 2004; RONQUIST et al. 2012a).

Two different Bayesian analyses were conducted, a time-free analysis (Fig. S2) and a time-calibrated analysis (Fig. S3). During the time-free analysis no further specifications were made following the input for reversible-jump MCMC. The MCMC generation settings included running 10 million generations, using four chains (three heated, one cold), with swap number set to one, and a temperature of 0.1 for the heated chains.

For the time-calibrated analysis a node dating approach was taken using the fossilized birth-death (FBD) macroevolutionary model (HEATH et al. 2014; ZHANG et al. 2016). Four constraints were specified across the tree for calibration: one at the root of the tree, representing the origin of the Gyrininae; one for the tribe Gyrinini, including all species in the genera *Aulonogyrus*, *Metagyrinus*, and *Gyrinus*; one for the ingroup taxa including all species of *Aulonogyrus*; and finally, a constraint for all species of *Gyrinus*. Each constraint represents either a currently (i.e. Gyrinini and *Aulonogyrus*, this study Fig. 1) or previously well supported monophyletic group (i.e. Gyrininae and *Gyrinus*: MILLER & BERGSTEN 2012; GUSTAFSON et al. 2017). Age estimates from GUSTAFSON et al. (2017) with offset exponential priors were used for calibration of these constraints (Table 1). An uncorrelated relaxed clock model IGR was selected with the rate vari-

Table 1. Node calibration constraints and settings used.

Calibration name	Min age	Mean age	Prior	Based on Gustafson et al. (2017) for …
root	151.52 Ma	174.95 Ma	Offset exponential	age of subfamily Gyrininae
Gyrinini	77.05 Ma	97.83 Ma	Offset exponential	age of tribe Gyrinini
Aulonogyrus	55.62 Ma	72.92 Ma	Offset exponential	age of *Aulonogyrus* + *Metagyrinus*
Gyrinus	57.88 Ma	76.48 Ma	Offset exponential	age of *Gyrinus*

ation prior across lineages set to exponential 10. As ages generated by the study from Gustafson et al. (2017), were used, the same clockrate prior estimated by the study for the family Gyrinidae was also used. As such, the sampling probability was set to 0.04 (or 38 species out of 900), as this clockrate prior was based on a phylogeny of the entire family Gyrinidae. Sampling strategy, which has previously been shown to strongly influence dating estimates under the FBD model (Gustafson et al. 2017), was set to diversity. The dating analysis was run under the same MCMC generation settings as above.

MCMC convergence of both the time-calibrated and time-free analyses was monitored using Tracer v.1.6 (Rambaut et al. 2014). A value of ESS ≥ 200 was considered as a good indicator of convergence.

Maximum likelihood. A maximum likelihood analysis was performed (Fig. S1) and implemented using the MPI version of IQ-Tree 1.5.5 (Nguyen et al. 2015). Again, the substitution model was not defined *a priori*, instead the command to allow ModelFinder (Kalyaanamoorthy et al. 2017) to find the model during analysis was used. For estimates of support, 1,000 replicates of ultrafast bootstrapping (Minh et al. 2013) were performed.

2.3. Ancestral Range Reconstruction

The time-calibrated tree (Fig. S3) from the Bayesian phylogenetic analysis was used for biogeographic inference with outgroup taxa pruned, except for *Metagyrinus sinensis* (Ochs, 1924) the sister taxon to *Aulonogyrus*. The program R and the package BioGeoBEARS (Matzke 2013a) was used to estimate the ancestral range of the genus *Aulonogyrus* across its entire distribution. This program offers several different models, including implementation of a parameter (+*j*) emulating founder-event jump speciation (Matzke 2013b, 2014). Analyses were run under the DEC (Ree et al. 2005; Ree & Smith 2008), DIVALIKE (Ronquist 1997), and BAYAREALIKE (Landis et al. 2013) models both with and without the +*j* parameter. Following completion of the analyses model fit was compared statistically in BioGeoBEARS.

The biogeographic regions used in the analysis were: Africa (A), Madagascar (M), Palearctic (P), Southeast Asia (S), and Oceania comprising Australia and New Caledonia (O) (Fig. 2). The geographic region assigned to each species is available in Table 1. Species were allowed to occupy a maximum of 3 geographic areas.

Three time strata were established for use in time-stratified analyses, these were: T1, 90–50 Ma; T2, 50–20 Ma; and T3, 20–present. T1 begins with Madagascar and India in relatively close proximity following India's separation and subsequent movement northward (Seton et al. 2012). At T2 the Indian plate has collided with the Eurasian plate leaving Madagascar isolated from all areas except Africa which has begun movement northward (Seton et al. 2012). During T3 Oceania becomes accessible to Southeast Asia as at least some land appeared in the region containing the present day Sunda chain as well as Wallacea (Hall 2013) and formation of major terrestrial area around New Guinea occurs facilitating biotic interchange (Toussaint et al. 2014). At this time the African plate has collided with the Eurasian plate bringing the Palearctic to its closest proximity to Africa, and Southeast Asia becomes more accessible to Africa via the Arabia peninsula (Seton et al. 2012).

Rate dispersal multipliers (Table S3) were applied to the three time strata using the following rules in reference to the global continental reconstructions of Seton et al. (2012). In regions largely separated by a small land or ocean barrier received a small rate penalty (dispersal rate, dr = 0.75), those separated by a medium ocean barrier or another biogeographic region had a medium rate penalty (dr = 0.50), and those separated by a large ocean and land barriers, as well as considerable distance received a large dispersal rate penalty (dr = 0.25). Finally, a conservative approach was taken for dispersal to regions considered to be under-water or appearing largely inaccessible due to considerable distance and the presence of multiple barriers. Dispersal to these regions was given a dispersal rate of 0.10 rather than zero, to account for the possibility of island refugia near areas considered underwater and long-distance dispersal.

3. Results

3.1. Phylogenetic analyses

Both the Bayesian and maximum likelihood analyses found strong support for the monophyly of *Aulonogyrus* (Figs. 1, S1–3), and considerably strong support for *Metagyrinus* as its sister, as has been found previously (Miller & Bergsten 2012; Gustafson et al. 2017). Within *Aulonogyrus*, the *Aulonogyrus* s.str. subgenus was strongly supported as monophyletic (Fig. 1: CI) and resolved as sister to the remaining species. The subgenus *Afrogyrus* was recovered in both Bayesian and maximum

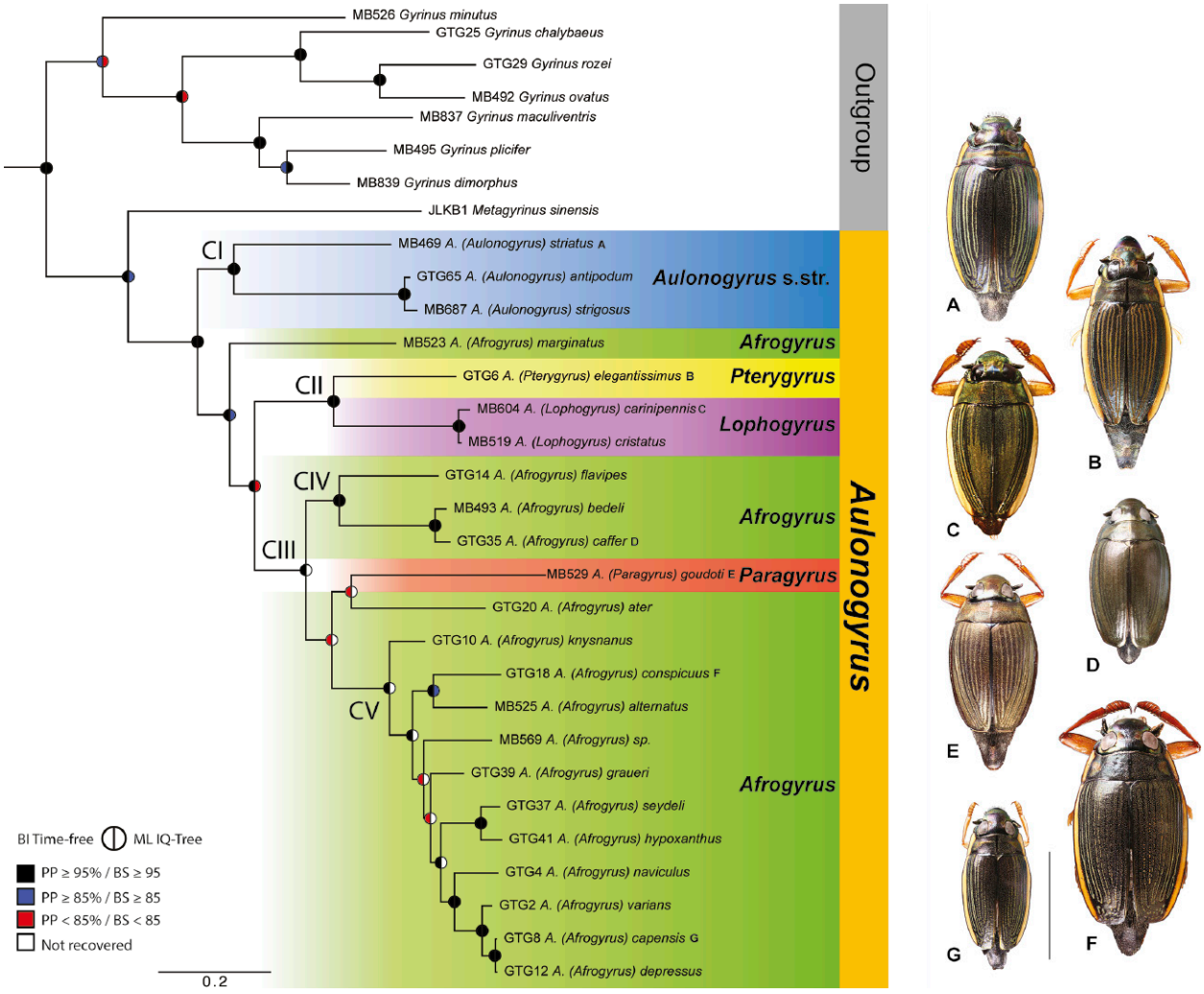

Fig. 1. Phylogenetic relationships of species of *Aulonogyrus*. The tree was recovered by time-free Bayesian inference (BI) (Fig. S2). The left half of the node denotes results from the time-free Bayesian analysis (Fig. S2), the right half shows results of the maximum likelihood analysis (Fig. S3). Color of the halves of the nodes shows support as indicated in the key at the bottom left. Bold letters next to dorsal habitus of species match letters next to terminal taxa in the phylogeny allowing for identification and showing phylogenetic placement. Scale bar for dorsal habitus images = 4 mm, all species to scale.

likelihood analyses as strongly paraphyletic with respect to the three previously proposed Malagasy subgenera (Fig. 1). The Bayesian analyses (Figs. S2, S3) strongly support *A. marginatus* (Aubé, 1838) as being sister to all other African and Malagasy species (posterior probability, pp = 1.00) with the next diverging clade composed of Malagasy species comprising the subgenera *Pterygyrus* and *Lophogyrus* (Fig. 1: CII) sister to a clade of African species with the only other Malagasy species, *A. goudoti* Régimbart, 1883 (Fig. 1E) nested well within it (pp = 0.98) (Fig. 1: CIII). The maximum likelihood analysis agreed with this configuration (Fig. S1), but with lesser support (superfast bootstrap support, bs = 88 and bs = 83). Both Bayesian and maximum likelihood analyses recovered all of the species present in clade III (Fig. 1: CIII) as each other's closest relatives, differing primarily in the placement of *A. goudoti* and *A. ater* Brinck, 1955a (Figs. S1, S2). The Bayesian analyses favored these two taxa as each other's sister, but with weak support (pp = 0.50 time-free, and pp = 0.61 time-calibrated); while maximum likelihood strongly favored *A. ater* as sister to the species within clade III (Fig. S1, bs = 100) with *A. goudoti* placed as sister to those species within clade V (Fig. S1, bs = 89). Neither of the two analyses recovered the dark-margined *Aulonogyrus* species as monophyletic (Figs. 1, S1–S3), but both found strong support for the monophyly of a small clade of dark-margined species (Fig. 2: CIV). Finally, both analyses agreed that all the species within clade V (Fig. 1: CV) were each other's closest relatives, differing primarily in the placement of *A. knysnanus* Brinck, 1955a and the sister species *A. seydeli* Ochs, 1954 + *A. hypoxanthus* Régimbart, 1906 (Figs. S1–S3).

3.2. Classification

The results of the phylogenetic analyses necessitate changes to the classification of the subgenera of *Aulonogyrus*, I propose the following changes (Fig. 2).

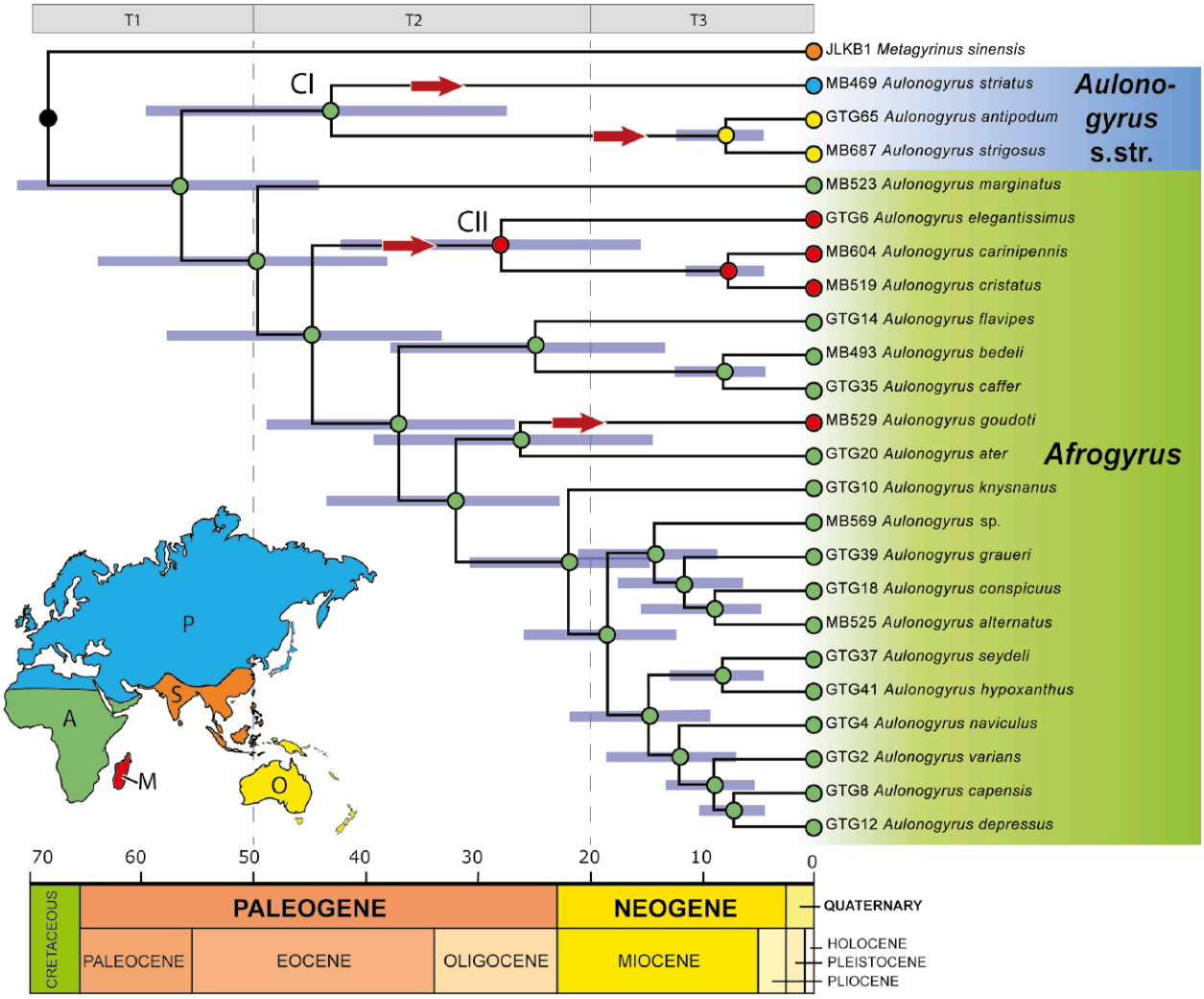

Fig. 2. Divergence times, historical biogeography, and proposed subgeneric classification of *Aulonogyrus*. The time-calibrated tree comes from Bayesian inference using a node calibrated approach under the fossilized birth-death model (Fig. S3). Blue bars at nodes denote the 95% hyperprior distribution for ages. T1–T3 show the three time strata established for the BioGeoBEARS analysis. Color at nodes indicate ancestral region reconstructed under the DEC model with > 50% probability (Fig. S5). Nodes that are black denote an ambiguous ancestral range reconstruction in which no area was recovered with > 50%. Color at tips show current species distribution. Red arrows indicate inferred dispersal events. The key in the bottom left shows definition of biogeographic regions and their corresponding colors.

Subgenus ***Aulonogyrus*** **s.str.** Motschulsky, 1853, type species *Gyrinus concinnus* Klug, 1834

Diagnosis. Labrum strongly strigose (Fig. 3A, lbr) (Brinck 1955a).

Composition. Four known species found in the Palearctic region, Australia, and New Caledonia.

Subgenus ***Afrogyrus*** Brinck, 1955a, type species *Gyrinus caffer* Aubé, 1838

Lophogyrus Brinck, 1955a, type species *A. carinipennis* Régimbart, 1895 **n.syn.**

Paragyrus Brinck, 1955a, type species *A. goudoti* Régimbart, 1883 **n.syn.**

Pterygyrus Brinck, 1955a, type species *A. elegantissimus* Régimbart, 1883 **n.syn.**

Diagnosis. Labrum not strongly strigose, at most weakly furrowed (as in *A. marginatus*) and most often completely smooth (Fig. 3B, lbr).

Composition. Fifty known species found primarily in Africa, with four from Madagascar, and one species (*A. obliquus* Walker, 1858) found in India and Sri Lanka.

3.3. Ancestral Range Reconstruction

For the ancestral range reconstruction, the DEC model was selected as the preferred model based on the corrected Akaike information criterion and weights (Table 2). The DEC models differed from the BAYAREALIKE and DIVALIKE reconstructions primarily in the ancestral range occupied by the common ancestor of all *Aulonogyrus*, and that for the common ancestor of the *Aulonogyrus* s.str. subgenus (Figs. S4–S15). However, these other models did not recover a single ancestral area for either node as being reconstructed with greater than 50% likelihood, suggesting ambiguous ancestral ranges, with the exception of the BAYAREALIKE +*j* model, which

Table 2. Results of the BioGeoBEARS analyses. — ***Abbreviations***: Lnl, logliklihood; #par, number of parameters; d, dispersal rate; e, extinction rate; j, jump dispersal rate; AICc, Akaike information criterion corrected; AICcwt, Akaike weight.

Model	LnL	#par	d	e	j	AICc	AICcwt
DEC	–15.69	2	0.011	0.17	0	35.96	0.59
DEC+J	–15.01	3	0.012	0.49	1.00E-05	37.21	0.31
DIVALIKE	–16.47	2	0.0001	0.0001	0.065	40.15	0.073
DIVALIKE+J	–17.53	3	0.001	0.0001	0.027	42.27	0.025
BAYAREALIKE	–29.20	2	0.0049	0.015	0.0001	65.59	2.20E-07
BAYAREALIKE+J	–21.45	3	1.00E-07	1.00E-07	0.1	50.09	0.0005

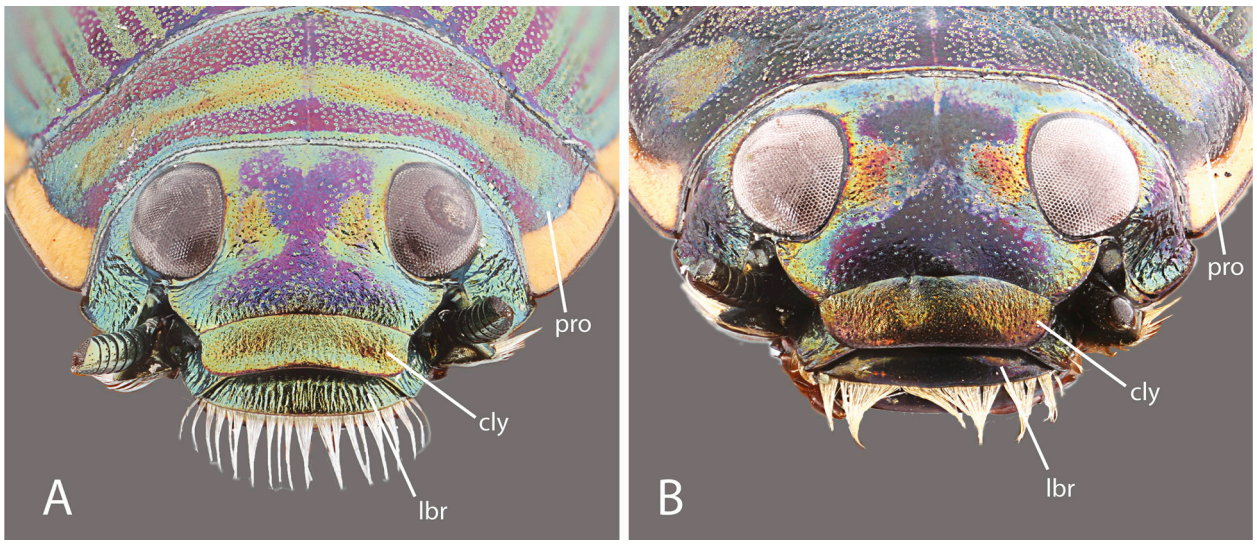

Fig. 3. Anterior view of head capsule showing labrum. **A**: *Aulonogyrus* (*Aulonogyrus*) *striatus* (Fabricius, 1792), showing diagnostic strigose labrum. **B**: *Aulonogyrus* (*Afrogyrus*) *conspicuus* Ochs, 1929, showing diagnostic smooth labrum. The metallic coloration is a genuine feature of the specimens. — ***Abbreviations***: cly, clypeus; lbr, labrum; pro, pronotum.

identified a Palearctic origin for both the genus *Aulonogyrus* and the subgenus *Aulonogyrus* s.str., with strong support (Fig. S15). The preferred ancestral range reconstruction (Fig. 2) under the DEC model favored an African origin for the common ancestor of all *Aulonogyrus*, as well as for both the *Aulonogyrus* s.str. and *Afrogyrus* subgenera. There are four independent Cenozoic dispersal events from out-of-Africa inferred by the DEC model (Fig. 2). Within the subgenus *Aulonogyrus* s.str. there are two dispersal events, one to the Palearctic (Fig. 2: CI) and another to Oceania. Within the subgenus *Afrogyrus* there are two separate dispersal events to Madagascar, the first being in the common ancestor of the species within clade II (Fig. 2: CII) and a second by the species *A. goudoti*.

4. Discussion

4.1. Phylogenetic relationships and classification

The results of the phylogenetic analyses found strong support for the monophyly of *Aulonogyrus* s.str., with the subgenus *Afrogyrus* being recovered as paraphyletic (Fig. 1) with respect to the Malagasy subgenera, which are here synonymized. The type species for *Afrogyrus* is *A. caffer* (Fig. 1D), thus another potential solution could be to synonymize *Pterygyrus* with *Lophogyrus*, as the monotypic *Pterygyrus* was based solely on automorphic features of *A. elegantissimus* (Fig. 1B), while maintaining *Lophogyrus* as a valid subgenus, as this clade (Fig. 1: CII) shares synapomorphic modifications to the elytra including one or more strongly keeled lateral elytral intervals and lateral elytral striae that run nearly to the elytral apex. Under this scenario *Afrogyrus* (including *Paragyrus*) would be defined primarily by lacking the diagnostic features of *Lophogyrus* (including *Pterygyrus*), as no distinct morphological synapomorphy has presented itself among this diverse clade of species. Furthermore, this solution would also require erecting a new subgenus for *A. marginatus*, which while possessing the vaguely unique feature of a weakly furrowed labrum (as opposed to being completely smooth as in other *Afrogyrus*, Fig. 3B, or strigose as in *Aulonogyrus* s.str., Fig. 3A), is so similar in gross anatomy to other members of *Afrogyrus*, BRINCK (1955a) placed it in a species-group that includes species from clade CV (Fig. 1: CV) (i.e. *A. knysnanus*, *A. graueri*, *A. naviculus* and *A. varians*), which is nested well within *Afrogyrus*. Therefore, I found the most prudent solution (Fig. 2) to be synonymization

of all Malagasy subgenera with *Afrogyrus* without erecting a new subgenus for *A. marginatus*, as this makes *Afrogyrus* a strongly supported monophyletic subgenus with the morphological synapomorphy of strongly reduced labral strigosity serving as a diagnostic feature for the subgenus (Fig. 3B).

4.2. Evolution and historical biogeography of *Aulonogyrus*

The results of the ancestral range reconstruction provide strong support for the long-standing hypothesis that *Aulonogyrus* originated within the Ethiopian region (Hatch 1926; Ochs 1949; Brinck 1955a,b). While the Australasian species were reconstructed as members of a clade sister to all other *Aulonogyrus* (Fig. 2: CI), the biogeographic analyses primarily supported an African origin for this group with subsequent Cenozoic dispersal to the Oceania region. This Cenozoic out-of-Africa dispersal scenario is very similar to the historical biogeography of the pond skater genus *Limnogonus* Stål, 1868 (Hemiptera, Gerridae) (Ye et al. 2016), another aquatic insect that lives on the surface of freshwater. The ancestral range reconstruction also revealed at least two independent dispersal events to Madagascar (Fig. 2). The earlier of these dispersal events resulted in a small clade of endemic species (Fig. 2: CII) with very unique morphology (Fig. 1B,C). Contrary to the proposed hypothesis that dark-margined, lentic *Aulonogyrus* species represented the earliest diverging lineages within the genus, these species were recovered as being nested within the subgenus *Afrogyrus* (Fig. 1: CIV and *A. goudoti* + *A. ater*). Furthermore, the results of the phylogenetic analyses support Brinck's (1955a) hypothesis that the dark-margined species do not form a natural group, and that yellow margins evolved and/or were lost multiple times within the genus.

5. Conclusions

This study revealed the historical biogeography of *Aulonogyrus* to be shaped primarily by Cenozoic dispersal out-of-Africa (Fig. 2). The ancestral range reconstruction strongly supported the previously proposed hypothesis that the genus originated within the Ethiopian region, specifically mainland Africa (Fig. 2). No support was found for a Gondwanan vicariance scenario. The phylogenetic analyses (Fig. 1) provided strong support for the monophyly of the *Aulonogyrus* s.str. subgenus, but required synonymy of most of the previously proposed subgenera (Brinck 1955a) with the subgenus *Afrogyrus*. Members of *Afrogyrus* can now be diagnosed as species having strongly reduced labral strigosity, with the labrum either appearing weakly furrowed or completely smooth (Fig. 3B). This new classification will provide improved nomenclatural stability as both subgenera as currently defined are strongly supported as monophyletic (Figs. 1, 2).

6. Acknowledgements

I greatly appreciate colleagues providing molecular-grade specimens for use in this study, particularly Stephen Baca who provide many valuable species from Kenya, Kelly Miller and Johannes Bergsten for South African specimens, Robert Sites for additional African specimens, Marianna Simões for *Gyrinus chalybaeus*, and very special thanks are due to Manfred Jäch for providing specimens of the extremely rare *A. antipodum* from New Caledonia. Andrew E.Z. Short is also thanked for his comments and edits improving this manuscript. I am supported by a NIH IRACDA postdoctoral fellowship (5K12GM064651).

7. References

Brinck P. 1955a. A revision of the Gyrinidae (Coleoptera) of the Ethiopian region. I. – Lunds Universitets Årsskrift. N.F. Avd. 2 **51**: 1–144.

Brinck P. 1955b. A monograph of the whirligig beetles of southern Africa. Pp. 329–518 in: Hanström B., Brink P., Rudebeck G. (eds), South African Animal Life. – Almqvist Wiksel, Stockholm.

Colgan D.J., Mclauchlan A., Wilson G.D.F., Livingston S.P., Edgecombe G.D., Macaranas J., et al. 1998. Histone H3 and U2 snRNA DNA sequences and arthropod molecular evolution. – Australian Journal of Zoology **46**: 419–437.

Edgar R.C. 2004. MUSCLE: multiple sequence alignment with high accuracy and high throughput. – Nucleic Acid Research **32**: 1792–1797.

Gustafson G.T., Prokin A.A., Bukontaite R., Bergsten J., Miller K.B. 2017. Tip-dated phylogeny of whirligig beetles reveals ancient lineage surviving on Madagascar. – Scientific Reports **7**: 8619.

Hall R. 2013. The palaeogeography of Sundaland and Wallacea since the Late Jurassic. – Journal of Limnology **72**: 1–17.

Hatch M.H. 1926. The phylogeny and phylogenetic tendencies of Gyrinidae. – Papers of the Michigan Academy of Science, Arts and Letters **5** (1925): 429–467.

Heath T.A., Huelsenbeck J.P., Stadler T. 2014. The fossilized birth-death process for coherent calibration of divergence-time estimates. – Proceedings of the National Academy of Sciences **111**: E2957–E2966.

Huelsenbeck J.P., Larget B., Alfaro M.E. 2004. Bayesian phylogenetic model selection using reversible jump Markov Chain Monte Carlo. – Molecular Biology and Evolution **21**: 1123–1133.

Kalyaanamoorthy S., Minh B.Q., Wong T.K.F., von Haeseler A., Jermiin L.S. 2017. ModelFinder: fast model selection for accurate phylogenetic estimates. – Nature Methods **14**: 587–589.

Landis M.J., Matzke N.J., Moore B.R., Huelsenbeck J.P. 2013. Bayesian analysis of biogeography when the number of areas is large. – Systematic Biology **62**: 789–804.

Lanfear R., Calcott B., Ho S., Guindon S. 2012. PartitionFinder: combined selection of partitioning schemes and substitution models for phylogenetic analysis. – Molecular Biology and Evolution **29**: 1695–1701.

Legros C. 1951. Les gyrins de Madagascar (Coléoptères). – Le Naturaliste Malgache **3**: 117–123.

Maddison W.P., Maddison D.R. 2015. Mesquite: a modular system for evolutionary analysis. Version 3.04. – Available at http://mesquiteproject.org/ [accessed on 12 September 2016].

Matzke N.J. 2013a. BioGeoBears: BioGeography with Bayesian (and Likelihood) Evolutionary Analysis in R Scripts. R package, version 0.2.1. – Available at http://cran.r-project.org/package=BioGeoBEARS [accessed on 5 January 2018].

Matzke N.J. 2013b. Probabilistic historical biogeography: new models for founder-even speciation, imperfect detection, and

fossils allow improved accuracy and model-testing. – Frontiers of Biogeography **5**: 242–248.

MATZKE N.J. 2014. Model selection in historical biogeography reveals that founder-event speciation is a crucial process in island clades. – Systematic Biology **63**: 951–970.

MAZZOLDI P. 2010. Gyrinidae (Coleoptera). Pp. 31–43 in: JÄCH M., BALKE M. (eds), Water Beetles of New Caledonia (part 1). – Zoologisch-Botanische Gesellschaft, Section of Entomology, Vienna.

MILLER K.B., BERGSTEN J. 2012. Phylogeny and classficiation of whirligig beetles (Coleoptera: Gyrinidae): relaxed-clock model outperforms parsimony and time-free Bayesian analyses. – Systematic Entomology **37**: 705–746.

MINH B.Q., NGUYEN M.A.T., VON HAESELER A. 2013. Ultrafast approximation for phylogenetic bootstrap. – Molecular Biology and Evolution **30**: 1188–1195.

NGUYEN L.-T., SCHMIDT H.A., VON HAESELER A., MINH B.Q. 2015. IQ-TREE: a fast and effective stochastic algorithm for estimating maximum likelihood phylogenies. – Molecular Biology and Evolution **32**: 268–274.

OCHS G. 1949. A revision of the Australian Gyrinidae. – Records of the Australian Museum **22**: 171–199.

RAMBAUT A., SUCHARD M., XIE D., DRUMMON A.J. 2014. Tracer v1.6. – Available at http://tree.bio.ed.ac.uk/software/tracer/ [accessed on 10 November 2015].

REE R.H., MOORE B.R., WEBB C.O., DONOGHUE M.J. 2005. A likelihood framework for inferring the evolution of geographic range on phylogenetic trees. – Evolution **59**: 2299–2311.

REE R.H., SMITH S.A. 2008. Maximum likelihood inference of geographic range evolution by dispersal, local extinction, and cladogensis. – Systematic Biology **57**: 4–14.

RÉGIMBART M. 1883. Essai monographique de la famille des Gyrinidae. 2e partie. – Annales de la Société Entomologique de France **6**: 121–190 + pl. 6.

RONQUIST F. 1997. Dispersal-vicariance analysis: a new approach to the quantification of historical biogeography. – Systematic Biology **46**: 195–203.

RONQUIST F., KLOPFSTEIN S., VILHELMSEN L., SCHULMEISTER S., MURRAY D.L., RASNITSYN A.P. 2012a. A total-evidence approach to dating with fossils, applied to the early radiation of Hymenoptera. – Systematic Biology **61**: 973–999.

RONQUIST F., TESLENKO M., VAN DER MARK P., AYRES D.L., DARLING A., HÖHNA S., LARGET B., LIU L., SUCHARD M.A., HUELSENBECK J.P. 2012b. MrBayes version 3.2: efficient Bayesian phylogenetic inference and model choice, across a large model space. – Systematic Biology **61**: 539–542.

SETON M., MÜLLER R.D., ZAHIROVIC S., GAINA C., TORSVIK T., SHEPHARD G., TALSMA A., GURNIS M., TURNER M., MAUS S., CHANDLER M. 2012. Global continental and ocean basin reconstructions since 200 Ma. – Earth-Science Reviews **113**: 212–270.

SIMON C., FRATI F., BECKENBACH A., CRESPI B., LIU H., FLOOK P. 1994. Evolution, weighting, and phylogenetic utility of mitochondrial gene sequences and a compilation of conserved polymerase chain reaction primers. – Annals of the Entomological Society of America **87**: 651–701.

SVENSON G.J., WHITING M.F. 2004. Phylogeny of Mantodea based on molecular data: Evolution of a charismatic predator. – Systematic Entomology **29**: 359–370.

TOUSSAINT E.F.A., HALL R., MONAGHAN M.T., SAGATA K., IBALIM S., SHAVERDO H.V., VOGLER A.P., PONS J., BALKE M. 2014. The towering orogeny of New Guinea as a trigger for arthropod megadiversity. – Nature Communications **5**: 4001.

WATTS C., HAMON H. 2010. Pictorial Guide to the Australian Whirligig Beetles. – Entomology Department, South Australian Museum. Available at http://www.samuseum.sa.gov.au/Upload/Files-Biological-Sciences/Terr-Inverts-text/Guide_to_Gyrinidae-branded.pdf [accessed on 5 January 2018].

WHITING M.F. 2002. Mecoptera is paraphyletic: multiple genes and phylogeny of Mecoptera and Siphonaptera. – Zoologica Scripta **31**: 93–104.

WILD A.L., MADDISON D.R. 2008. Evaluating nuclear protein-coding genes for phylogenetic utility in beetles. – Molecular Phylogenetics and Evolution **48**: 877–891.

YE Z., ZHEN Y., ZHOU Y., BU W. 2016. Out of Africa: Biogeography and diversification of the pantropical pond skater genus *Limnogonus* Stål, 1868 (Hemiptera: Gerridae). – Ecology and Evolution **7**: 793–802.

ZHANG C., STADLER T., KLOPFSTEIN S., HEATH T.A., RONQUIST F. 2016. Total-evidence dating under the fossilized birth-death process. – Systematic Biology **65**: 228–249.

Electronic Supplement File

at http://www.senckenberg.de/arthropod-systematics

File 1: gustafson-aulonogyrusphylogeny-asp2018-electronicsupplement.pdf — **Table S1.** Taxon sampling and gene coverage as indicated by GenBank voucher numbers for phylogenetic analyses, including biogeographic range coding for ancestral state reconstruction in BioGeoBears. See Fig. 2 for which area the coded character represents. — **Table S2.** Primers used for amplification and sequencing. — **Table S3.** Dispersal rate multipliers used in BioGeoBEARS ancestral range reconstruction. — **Fig. S1.** Results of maximum likelihood phylogenetic analysis using IQ-Tree. Numbers at nodes indicate superfast bootstrap support. — **Fig. S2.** Results of time-free Bayesian phylogenetic inference using MrBayes. Numbers at nodes indicate posterior probability support. — **Fig. S3.** Results of time-calibrated Bayesian phylogenetic inference using a node-calibrated approach under the FBD model in MrBayes. Numbers at nodes indicate posterior probability support. Colored bars show 95% hyperprior distribution for age. — **Fig. S4.** BioGeoBEARS DEC model results, nodes with most probable ancestral state indicated. — **Fig. S5.** BioGeoBEARS DEC model results, nodes with pie chart of relative ancestral state probabilities. — **Fig. S6.** BioGeoBEARS DEC+J model results, nodes with most probable ancestral state indicated. — **Fig. S7.** BioGeoBEARS DEC+J model results, nodes with pie chart of relative ancestral state probabilities. — **Fig. S8.** BioGeoBEARS DIVALIKE model results, nodes with most probable ancestral state indicated. — **Fig. S9.** BioGeoBEARS DIVALIKE model results, nodes with pie chart of relative ancestral state probabilities. — **Fig. S10.** BioGeoBEARS DIVALIKE+J model results, nodes with most probable ancestral state indicated. — **Fig. S11.** BioGeoBEARS DIVALIKE+J model results, nodes with pie chart of relative ancestral state probabilities. — **Fig. S12.** BioGeoBEARS BAYAREALIKE model results, nodes with most probable ancestral state indicated. — **Fig. S13.** BioGeoBEARS BAYAREALIKE model results, nodes with pie chart of relative ancestral state probabilities. — **Fig. S14.** BioGeoBEARS BAYAREALIKE+J model results, nodes with most probable ancestral state indicated. — **Fig. S15.** BioGeoBEARS BAYAREALIKE+J model results, nodes with pie chart of relative ancestral state probabilities.